Graphene oxide/vinyl ester resin nanocomposite: the effect of graphene oxide, curing kinetics and mechanical properties

V. Arabli* and A. Aghili**

*Department of Polymer Engineering, Shiraz Branch
Islamic Azad University, Shiraz, Iran, arably@yahoo.com
**Department of Polymer Engineering, Shiraz Branch
Islamic Azad University, Shiraz, Iran, aghili@iaushiraz.ac.ir

ABSTRACT

Graphene oxide (GO) was synthesized and nanocomposites were prepared using different contents of the GO and vinyl ester resin (VE). The nonisothermal differential scanning calorimetry (DSC) was used to study the cure kinetics of VE and 0.3wt% GO/VE nanocomposite. Kissinger and Ozawa equations were used to determine the activation energy (Ea). The Ea values of the cured GO/VE nanocomposite showed a decrease with respect to the neat VE. It is concluded that GO has a catalytic effect in the cure reaction. The dynamic curing process was modeled to predict the degree of curing and curing rate of resin. Scanning electron microscopy (SEM) was studied to discern the surface features and dispersion of GO. The glass transition temperature (Tg) was obtained from the maximum peak temperature of the loss factor curve. The Tg was increased by nearly 10 °C by the addition of 0.4 wt% GO to VE. Tensile mechanical tests were studied and the nanocomposite of 0.3 wt% GO/VE showed higher elongation and tensile strength.

Keywords: Graphene Oxide; Epoxy Vinyl Ester Resin; Cure Kinetics; Mechanical properties.

1 INTRODUCTION

Vinyl ester resins are thermoset matrices that are widely used in the composites industry [1]. VE resin is produced by the esterification of epoxy resin with unsaturated monocarboxylic acid. The resins are widely used in environments that require high corrosion and chemical resistance, water barrier properties, low moisture absorption, low shrinkage and good dimensional stability [2]. Generally, these resins have been used in a range of applications as a matrix material, coating, wide adhesive, electronic encapsulant, in the marine industry, pipelines and automotives [3]. The thermoset epoxy polymers can be mixed with a second phase of nanofillers such as nanospheres, nanotubes, nanoplatelets, etc. These nanocomposites improve the toughness, stiffness, strength and thermal properties. As a layered carbon nanomaterial, graphene with high aspect ratios is widely used to improve mechanical, thermal and electrical properties in polymer materials. However, the high cost and poor dispersion of the CNTs and CNFs in the polymers, limits the range of practical application [4].

2 EXPERIMENTAL

2.1 Materials

Natural graphite flakes (100 meshes) were supplied by Sigma-Aldrich (Saint Louis, USA). V301 epoxy (VE) using bisphenol A epoxy was purchased from Farapol (Hamadan, Iran). Cobalt, dimethylaniline (DMA) and methyl ethyl ketone peroxide (MEKP), sulfuric acid (H2SO4), phosphoric acid (H3PO4), potassium permanganate (KMnO4), hydrogen peroxide (H2O2), hydrochloric acid (HCl), tetrahydrofuran (THF) solvent and other chemicals were purchased from Merck Chemicals Company.

2.2 Devices and Equipment

DSC was measured by a Mettler Toledo. SEM images were taken by a TESCAN Vega TS 5136mm. XRD was measured using a Bruker D/Max2550 V X-ray diffractor. A UP400S sonicator (Hielscher, DE) was used for dispersion of graphene oxide in the GO/VE nanocomposite.

2.3 Synthesis and Preparation of GO

The improved method of Hummers [5] was used to prepare GO from graphite flakes. For this purpose, a mixture of concentrated H2SO4/H3PO4 (360 : 40 mL) was added gradually with stirring to a mixture of graphite flakes/KMnO4 (3 : 18 g). Then, the reaction was warm up to 45 °C and mixed for 12 h. The reaction was cooled and poured onto 400 g ice with 3mL of 30% hydrogen peroxide. The mixture was sifted through a metal sieve and then filtered. The filtrate materials were centrifuged at4000 rpm for 4 h, and solid product was separated. The solid product was then washed with 200 mL of water, 200 mL of 30% HCl, and 200 mL of ethanol, respectively. After each wash, the mixture was then purified following the previous protocol of sifting, filtering and centrifugation. The material remaining was coagulated with 200 mL of ether, and the mixture was filtered again. The resulting GO obtained on the filter was vacuum dried overnight at room temperature to produce the GO powder. The resulted GO was placed into a crucible, and the crucible was put into a furnace

(preheated to 1050 °C for 30 s) to obtain the graphene.

2.4 Preparation of GO/VE Nanocomposite

Different weight contents of GO (0.1, 0.3, 1.5, 3.0 wt%) were first ultrasonicated in 50 mL of THF solvent for 1 h. The homogeneous solution of GO, in THF, was then mixed with 100 g VE monomer. The mixture stirred and ultrasonicated, for 30 min. The mixture was degassed at 60 °C in a vacuum oven for10 h. Afterwards, 1.5 mL MEKP and 0.3% cobalt were added and the mixture stirred again. Then, the cured sample were pre-cured in an oven at 80°C for 2 h and post-cured at 120 °C for another 1 h.

2.5 DSC and TGA

25 mg of the uniform viscous mixture was put in the DSC sample cell at room temperature. The sample was heated by constant heating rate (5, 10 and 15 °C /min) from 25 to 160 °C under nitrogen gas flow of 22 ml/min. Degradation and weight loss of the VE and its nanocomposite was investigated by the TGA system under nitrogen gas flow of 22 ml/min and heating rate of 10 °C/min.

3 RESULTS AND DISCUSSION

3.1 XRD Evaluation

XRD patterns of graphite, graphene oxide and GO/VE nanocomposite are shown in Fig. 1. The peak at $2\theta = 26.55$ for graphite corresponds to the diffraction of the (002) graphite plane composed to an interlayer spacing of 0.355 nm [6]. The peak at $2\theta = 9.45$ (graphene oxide) corresponds to the diffraction of the (002) graphite oxide plane. The interlayer spacing of the graphite oxide can be obtained according to Bragg's law: $n\lambda = 2d \sin\theta$
where n is the diffraction series, λ is the X-ray wavelength, and d is the interlayer spacing of graphene oxide. The calculated value of d (0.935 nm), implies that the sample is expanded when graphite is oxidized. However, this peak has disappeared in graphene, indicating that the distances between the graphene layers have been greatly expanded and the layers are disordered [7].

3.2 Curing Kinetics and Modeling

Non-isothermal (DSC) was used to study the kinetics of the cure reaction of VE and its nanocomposite. The results are shown in Fig. 2. The values of peak temperatures and heats of reaction are shown in Table 1. All kinetic models have a same basic equation:

$$\frac{d\alpha}{dt} = k(T) f(\alpha) \qquad (1)$$

where $d\alpha/dt$ is the cure reaction rate, $k(T)$ is the rate constant, α is the fractional conversion at a time t, $f(\alpha)$ is function of α. A kinetic model for a dynamic curing process with a constant heating rate can be explained as [8]:

$$\frac{d\alpha}{dt} = Ae^{-Ea/RT}\alpha^m(1-\alpha)^n \qquad (2)$$

where $k(T)$ and $f(\alpha)$ are replaced by Arrhenius equation and an equation based on an autocatalytic model, respectively. A is the pre-exponential factor, E_a is the activation energy, R is the gas constant, and T is the absolute temperature. The correlation between $d\alpha/dt$ and $d\alpha/dT$ can be explained:

$$\frac{d\alpha}{dt} = \left(\frac{dT}{dt}\right)\frac{d\alpha}{dT} \qquad (3)$$

where dT/dt is constant heating rate. Substituting Eq. (2) and (3) gives:

$$\frac{d\alpha}{dT} = A\left(\frac{dT}{dt}\right)^{-1}\alpha^m(1-\alpha)^n \exp\left(\frac{-Ea}{RT}\right) \qquad (4)$$

Following form is general linear eq. between the heating rate and peak temperature T_p as Ozawa [9] method:

$$\ln\left(\frac{dT}{dt}\right) = c + \left(\frac{-Ea}{R}\right)\left(\frac{1}{T}\right) \qquad (5)$$

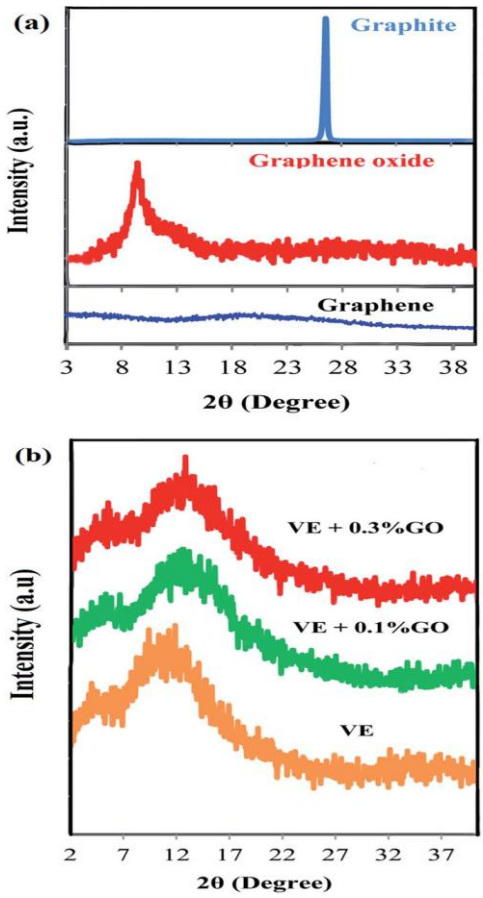

Fig. 1: XRD patterns of (a) graphite, graphene oxide, and graphene, (b) neat VE and its composites containing different contents of GO.

Sample	VE			VE + 0.3% GO		
q (°C /min)	5	10	15	5	10	15
T_p (K)	350.15	363.65	372.55	351.15	366.45	374.25
Exo. Heat (J/g)	65.06	65.13	61.84	71.18	66.12	63.98

Table 1: Dynamic DSC data for the curing of resin at different heating rates.

Sample	VE	VE + 0.3% GO
Ea [a](kj/mol)	56.6	43.6
Ea [b](kj/mol)	59.8	49.0

[a] Kissinger method, [b] Ozawa method

Table 2: E_a values from Kissinger and Ozawa methods.

Equation (6) indicates Kissinger eq. [10].

$$-\ln\left(\frac{q}{T_p^2}\right) = \frac{Ea}{R\,Tp} - \ln\left(\frac{AR}{Ea}\right) \qquad (6)$$

where q is the heating rate. A plot of $\ln(q/T_p^2)$ versus $1/T_p$ was made as a Kissinger plot and also $\ln(q)$ versus $1/T_p$ was made as an Ozawa plot for peaks of the individual DSC curves. Values of activation energies for each peak are shown in Table 2. By comparing the Ea for both systems of resin (VE and VE + 0.3% GO), it can be suggested that GO as a catalyst, improved the cure reaction and decreased Ea values.

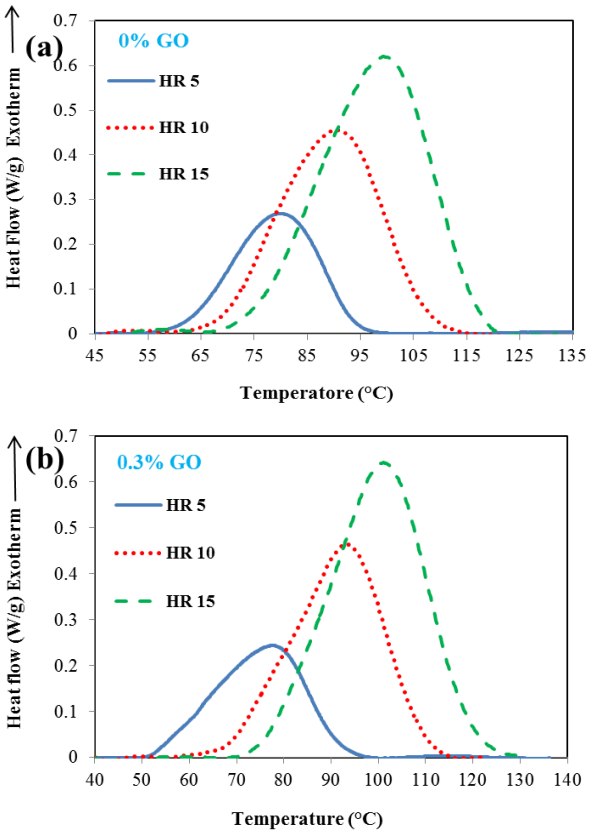

Figure 2: DSC curves (a) VE (b) VE + 0.3% GO.

3.3. Dynamic mechanical properties (DMA)

Information on the storage modulus and loss factor (tan delta) of a cured resin and its composites can be measured by dynamic mechanical analysis (Fig. 3a and b) [11]. As shown in Fig. 3a, the incorporation of GO sheets leads to an increase of the storage modulus in the whole temperature range. This can be well explained by the reinforcing effect of the nano-filler leading to an increase of stiffness. The increase of storage modulus is due to the nanofiller reinforcement and the mobility restriction of the matrix chains induced by the formed covalent bonds between the epoxy matrix and the sheets. The tan delta value is the ratio of the loss modulus to the storage modulus, and the peak of tan delta is often used to obtain the Tg. The Tg values of GO/VE composites are listed in Table 3. As shown in Table 3 and, Fig. 3b the Tg of the GO/VE composites has shifted to a higher temperature compared with that of neat VE. The storage moduli of the composites show increase with the sheet weight loading. The wrinkled morphology of graphene oxide sheets with high specific surface area is speculated to constrain the segmental movement of matrix chains to a certain degree. Therefore, these results slightly increase the Tg value.

3.4. Tensile mechanical tests and fracture surface analysis of cured nanocomposites

Typical stress–strain curves of VE and its composites with different filler loadings are shown in Fig. 4a. The tensile properties are listed in Table 3. As shown in Fig. 4a and b the highest increase in tensile strength is almost 38% (from 63.03 to 87.08 MPa) at a GO loading of 0.30 wt%. Further increase in GO content impairs tensile strength slightly. Similarly, the elongation at break shows an increase at a loading of 0.30 wt% and then decreases with further increase of the GO content (Fig. 4c). It can be observed that the tensile strength of the VE depends on the percent of GO. With increasing graphene oxide, the vinyl ester resin becomes harder to break, thus the samples with a higher percent of GO show more tensile strength. However, the GO/VE nanocomposite prepared with 0.3% GO shows higher elongation and tensile strength than the GO/VE prepared with 0.4% GO. The decrease of tensile strength with a higher percent of GO may be attributed to poor linkage, weak interface, and micro bubbles formed between the resin matrix and GO.

4 CONCLUSION

Effect of GO on the cure kinetics of VE in the presence of 0.3% wt GO was studied. To determine activation energy of the cure reaction of VE, non-

isothermal DSC method, Ozawa and Kissinger equations were used. The Ea value of cure reaction of VE in the presence of 0.3% GO decreased. It is concluded that GO acted as catalyst in the reaction of VE/GO. The Tg was increased by the addition of 0.4 wt% GO to VE. Tensile mechanical tests were studied and the nanocomposite of 0.3 wt% GO/VE showed higher elongation and tensile strength.

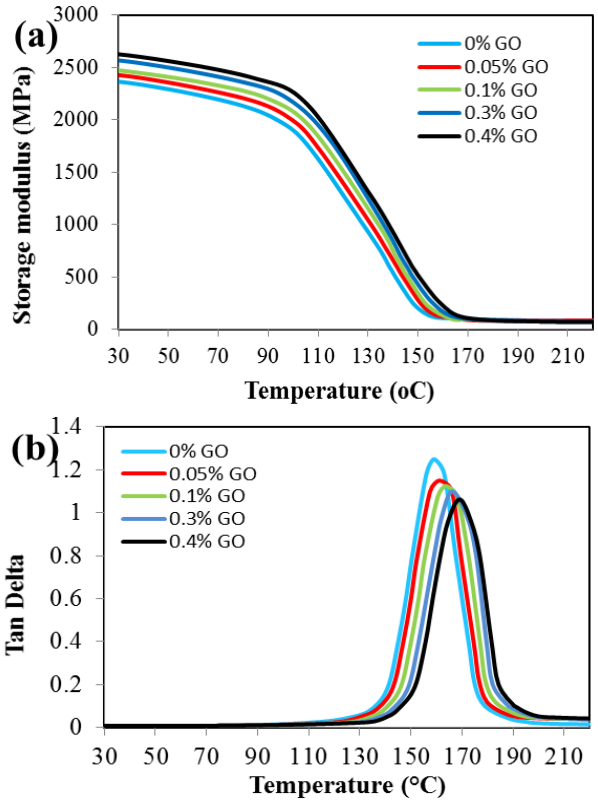

Figure 3: Dynamic mechanical properties of neat VE and its composites: (a) storage modulus and (b) tan delta.

Sample	Tensile Strength (MPa)	Elongation at Break (%)	T_g (°C)
Neat VE	63.03 ± 5.03	3.99 ± 0.44	159.0
VE + 0.05% GO	68.15 ±4.88	4.18 ± 0.64	161.1
VE + 0.1% GO	80.30 ± 5.14	5.46 ± 0.69	163.5
VE + 0.3% GO	87.08 ± 5.33	5.91 ± 0.39	166.2
VE + 0.4% GO	84.10 ± 5.10	5.72 ± 0.55	169.1

Table 3: Mechanical and thermal properties of neat VE and its composites with different filler loadings

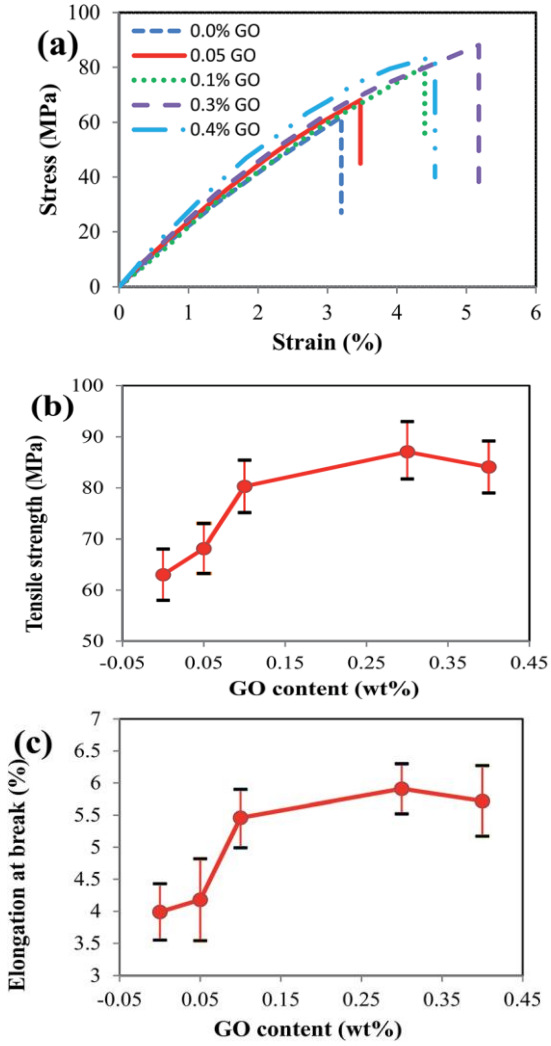

Figure 4: Tensile properties of neat VE and its composites with different filler loadings: (a) stress–strain curves, (b) tensile strength, (c) elongation at break.

REFERENCES

[1] C. Jang, T. E. Lacy, S. R. Gwaltney, H. Toghiani and C. U. Pittman, Macromolecules, 45, 4876, 2012.
[2] A. Chaturvedi and A. Tiwari, Adv. Mater. Lett., 4, 656, 2013.
[3] X. Zhang, V. Bitaraf, S. Wei and Z. Guo, AIChE J., 60, 266, 2014.
[4] Z. Wang, P. Wei, Y. Qian and J. Liu, Composites, Part B, 60, 341, 2014.
[5] W. S. Hummers and R. E. Offeman, J. Am. Chem. Soc., 80, 1339, 1958.
[6] H.-K. Jeong, Y. P. Lee, R. J. W. E. Lahaye, M.-H. Park, K. H. An, I. J. Kim, C.-W. Yang, C. Y. Park, R. S. Ruoff and Y. H. Lee, J. Am. Chem. Soc., 130, 1362, 2008.
[7] D. A. Nguyen, Y. R. Lee, A. V. Raghu, H. M. Jeong, C. M. Shin and B. K. Kim, Polym. Int., 58, 412, 2009.
[8] L. Sun, S. S. Pang, A. M. Sterling, I. I. Negulescu, M. A. Stubblefield, J. Appl. Polym. Sci. 86, 1911, 2002.
[9] T. J. Ozawa, Therm. Anal. 2, 301, 1970.
[10] H. E. Kissinger, Anal. Chem. 29, 1702, 1957.
[11] Q. Feng, X.-J. Shen, J.-P. Yang, S.-Y. Fu, Y.-W. Mai and K. Fried, Polymer, 52, 6037, 2011.